Narrow Canyon Effect on the Behavior of Earth Dams at the End of Construction (Case Study: Vanyar Dam)

Mehdi Derakhshandi[1*], Mojtaba Honarmand[2], Amir Hossein Sadeghpour[3]

1. Department of Civil Engineering, Tehran Science and Research Brunch, Islamic Azad University, Tehran, Iran

2. Department of Civil Engineering, Arak University, Arak, Iran.

3. Department of Architecture and Art, University of Kashan, Kashan, Iran.

Received: 2021/2/21 Accepted: 2021/11/10

Abstract

Earth dams are geotechnical structures constructed on various shapes of a valley. The Vanyar Dam is a rock-fill dam located on a narrow valley. With respect to the geometry of the canyon, three-dimensional modeling was utilized in order to analyze this dam. The analysis was performed with FLAC3D software, which simulates geotechnical problems based on the finite difference method. The results show that the settlements obtained from numerical analysis are less than those recorded by the magnetic settlement devices, due to the lower compaction around them, which prevents damage to these instruments. According to the numerical analysis, the maximum settlement is 88.14 cm, which corresponds to 48 m above the bedrock in cross-section C, that is, a little less than 1% of the dam height. In addition, the total vertical stresses recorded by the pressure cells are about 28% less than those obtained from the numerical analysis. It is assumed that the difference is caused by local arching due to lower compaction and consequently a low stiffness area around the pressure cells. In terms of pore water pressure, there is good agreement between the pore water pressure obtained from the numerical analysis and the piezometers, such that the results are restricted to less than 1%. In general, the difference between the numerical analysis results

* Corresponding author: m-derakhshandi@ srbiau.ac.ir

and those recorded by the instruments are acceptable. Furthermore, the dam shows a suitable level of performance at the end of construction.

Keywords: Vanyar Dam; 3D Numerical Analysis; Narrow Canyon, Monitoring

1. Introduction

Among the most crucial types of engineering structures are earth dams, whose advantages include the flexibility of construction in the various geometries of valleys, the type of materials and the construction technology over other types of dams. When constructing these types of dams, it is necessary to deliver a safe design and a suitable level of performance, as well as install monitoring systems during construction and verify the numerical analysis results. Earth dams are usually constructed on wide (U-shape) valleys. Therefore, to analyze earth dams on a U-shape valley, two-dimensional (2D) numerical modeling, based on the plane strain, should be adopted as it typically offers sufficient precision.

Eisenstein et al. [1] stated that 2D numerical analysis of earth dams on a V-shape valley predicts settlements and stresses more effectively than three-dimensional (3D) numerical analysis.

Lefebvre et al. [2] carried out a series of finite element analyses on 2D and 3D models of earth dams. The results showed that, in a U-shape valley, the plane strain condition is a logical consideration, while 2D analysis somehow explains the mechanical behavior of such dams. Conversely, in a V-shape valley, this assumption is far from what occurs in reality, such that 3D modeling of the earth dam is required. In addition, 2-D modeling of an earth dam leads to appropriate results, provided that the length-to-height ratio of the earth dam is greater than six. Otherwise, it should be considered as 3-D modeling.

Belyakov [3] evaluated the effect of the length-to-height ratio of earth dams under various conditions. The study was carried out to evaluate the effect of the geometry of the valley and the earth dam on the results by considering 2D and 3D numerical analysis. The results demonstrated that the stress distribution and the form of arching in the earth dam are dependent on the length-to-height ratio, although the 3D effects on the results for earth dams with a height greater than 80 m and a shape factor greater than four can not be ignored.

Ohmachi [4] stated that the narrow valley has a significant effect on vibration of earth dam. In addition, fundamental period of earth dam will be shorter considerably when the length-to-height ratio is less than five.

Stark and Eid [5] showed that the difference in internal friction angle, which obtained from back analyses of 3D and 2D models of a slope, could reach to over 30%. Additionally, the factor of safety of 3D numerical analysis is greater compared to two-dimensional analysis.

Javaheri [6] carried out 2D and 3D static and dynamic numerical analyses on the rock-fill dam at Masjed Soleyman. The results showed that, in the middle cross-section, total vertical stress and maximum shear stress obtained from 2D analysis were respectively up to 15% and 30% more than 3D analysis in the same points. This was due to the transfer of stress to the abutments and the longitudinal arching in the 3D model. Consequently, it can be said that 2D numerical analysis is more conservative than 3D numerical analysis.

Heidari [7] showed that, for earth dams located in a valley with $\frac{L}{H} < 4$, plane strain analysis does not lead to precise results, which means that, in order to achieve accurate results, 3D numerical analysis is required.

Roth et al. [8] conducted 2D and 3D dynamic numerical analyses to evaluate the seismic performance of a stone canyon earth dam, located in a narrow canyon. The results showed that using a 2D plain strain model for short dams across narrow canyons lead to inherently conservative results, while using 3D analysis is more realistic.

Yu et al. ([9],[10]) conducted a parametric study on the effects of geometrical characteristics and the topography of a canyon on the stability of earth rock-fill dams. The results showed that canyon shape, length-to-height ratio of the earth rock-fill dam, gradient of the dam slope and height of the dam have a significant influence on the 3D slope stability of earth rock-fill dams. They further stated that the results of their study could be used as a blueprint for the 2D and 3D slope stability of dams.

Qu et al. [11] performed 2D and 3D numerical analyses on three earth dams respectively built on the St. Alban, Malaysia and Vernon embankments, which were constructed on a clayey foundation. These embankments were instrumented and the settlements of the embankments were monitored, with the results demonstrating that plane strain modeling of the embankments potentially lead to overestimation of available soil strength, although

this assumption is not accepted when designing embankments on a soft soil foundation. In addition, for embankments, 2D numerical analysis is recommended, provided that the base length-to-width ratio is greater than 2.

Mahinroosta et al. [12] proposed a constitutive model in order to simulate the nonlinearity of the rock-fill material behavior of the Gotvand Dam, due to its suitability for modeling the collapse settlement of rock-fill material during the first impoundment. Back analysis of the dam showed that the new constitutive model was more able to predict the collapse settlement values than instrumentation. This was due to the copious use of water during compaction of the rock-fill soil layers. In addition, the results indicated that using a lower rate of rising water during the first impoundment can help to decrease displacement values in the upstream shell.

Maddah et al. [13] compared the effect of clayey sand and pure clay properties on the behavior of earth dam cores in narrow valleys at the end of construction. They carried out a numerical stress-strain analysis on the longitudinal section of the centerline of earth dam at Masjed Soleyman in order to evaluate the impact of different types of material on deformation properties. The results demonstrated that shear stress is insensitive to certain types of material in cross-section valleys. Furthermore, the geometry and restraints of narrow valleys decrease the settlements and vertical stresses in the lower parts of dams.

Gurbuz and Peker [14] evaluated the monitoring system of the Karacasu Dam by focusing on the instrumentation results. They used the data from 18 earth pressure cells and 30 displacement cells embedded in the dam body, where were recorded by 15 joint meters installed on its concrete face. The results revealed that the effect of confinement and arching on the settlement led to the maximum settlement of the dam being equal to 1% of the height of the dam after construction. Furthermore, settlement and earth pressure recorded at several cross-sections of the dam were compared at two time periods, that is, the end of construction and when the maximum water level was reached.

A modified double-yield surface elastoplastic constitutive model was developed by Sukkarak et al. [15] to consider particle breakage for the purposes of the numerical analysis of high rock-fill dams. As a case study, 3D finite element modeling of the rock-fill Nam Ngum 2 Dam (182 m in height) was performed by using the model to predict the

settlements during the construction stage. The settlements calculated by the model had good agreement with those recorded by the instruments.

A summary and overview of various studies in this area show that, although there is no consensus on the limited value of the length-to-height ratio, other than for ratios greater than five, it can be deduced that 2D plane strain and 3D numerical analysis almost lead to the same results. Furthermore, 3D analysis should be conducted for ratios less than five. Indeed, the more the ratio is less than five, the more it is necessary to perform 3D analysis.

According to the literature, five is the maximum length-to-height ratio of earth dams in which 2D and 3D numerical analyses almost have the same results. The Vanyar Dam has been constructed on a narrow valley, whose length-to-height ratio is about three.

2D numerical analysis of the Vanyar Dam was carried out by Derakhshandi et al. [16]. The results showed a significant difference with the data recorded from instruments. They concluded that based on the geometry and shape of valley of the Vanyar Dam, it needs to use 3D modelling to reach a more accurate results.

By taking the ratio into account, 3D analysis is more appropriate for evaluating the static behavior of the dam at the end of construction. In this study, 3D numerical analysis of the Vanyar Dam was conducted and the results were compared with the data recorded by the instruments. The results concerning the settlements, total vertical stresses and pore water pressures were the outputs of numerical analysis, which were compared with those recorded by the monitoring system in the same points.

2. Engineering geology condition of the Vanyar Dam

In terms of engineering geology, the Vanyar Dam is located on thick layers of alluvium and debris material on the bedrock. This formation is due to geological nature of the site and the Ajichai riverbed. The oldest rocks around the dam axis, the Ajichai riverbed and the outcrop in the upstream area belong to the Upper Cretaceous period. The rocks are highly tectonized and have been affected by weathering and erosion factors to a great extent. These rocks include diabase formation (UB1), ultra-basic rocks (UB2), and shale, silicic, volcanic and sedimentary clastic Miocene unit sediments (Unit (M)). Fig. 1 presents the geological map of the dam site.

Except for the restricted crashed and tectonized zone, the rock masses of the dam abutments mainly have low permeability. Indeed, in the right abutment, permeability is less than 3 Lu at a depth of 14 m and below, whereas high permeability zones, in which Lugeon values are greater than 20, are located in depths less than 14 m. In the riverbed, the average Lugeon value is 23 in depths less than 13 m, whereas it decreases to 3 in depths below 13 m. In the left abutment, similar to the right abutment, the permeability is very low (less than 2 Lu at a depth of 25 m and below), whereas high permeability zones, in which Lugeon values are greater than 29, are located in depths less than 25 m. Based on RQD index data, the rock units at the dam abutments are classified as having very poor rock mass quality due to the presence of extreme crashed and tectonized rocks. The depth of weathered rocks is limited to 14 m, 13 m and 25 m for the right abutment, left abutment and riverbed, respectively. The average values of RQD for the left abutment, riverbed and right abutment are about 7%, 25% and 13.5%, respectively. In addition, the core of the dam was constructed on the bedrock by removing the highly permeable alluvium. Fig. 1 shows the engineering geology profile of the dam site. Furthermore, Mansouri et al. [17] studied the effect of salinity of the Ajichai-river on the mechanical behavior of sandstones in abutments and foundation of Vanyar dam. The results showed that saline water does not have a significant negative effect on the mechanical behavioral of sandstones. It should be noted that the specimens were tested about 300 days after the saturation of the specimens in saline water.

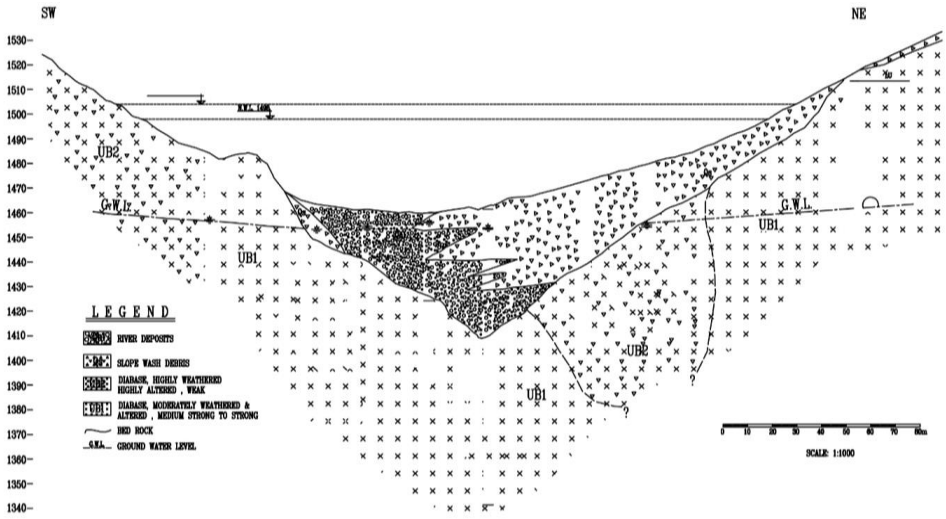

Fig. 1. Engineering geology profile of the dam site

3. Vanyar Dam specification and monitoring system

The Vanyar Dam is a rock-fill dam located on the Ajichai River approximately 5 km northeast of Tabriz. The dam site is located at longitude 46° 2′3 and latitude 38° 0′5 . Tabriz City is situated in very tectonized area with high seismicity, while the fault located in North Tabriz is about 5 km away from the dam site. The main reasons for constructing the dam were the agricultural water supply, desalination of water from the Ajichai River and flood control. The height of the dam is 91 m from the bedrock and 39 m from the riverbed. Therefore, 52 m were excavated from the riverbed in order to construct the dam on the bedrock. The transient shell is located between the filter and the rock-fill shell, while a riprap layer protects the upstream shell. A two-layer filter protects the core in the upstream and downstream areas. Fig. 2 presents the downstream view of the Vanyar Dam at the end of construction. Table 1 sets out the technical specification of the dam.

Fig. 2. Downstream view of Vanyar Dam at the end of construction

Table 1: Technical characteristics of the Vanyar Dam and its reservoir [18]

Dam information	Value
Height of crest from bedrock	91 m
Height of crest from riverbed	39 m
Dam crest elevation a.s.l.	1,504 m
Normal water level a.s.l.	1,498 m
Length of dam crest	278 m
Width of dam crest	10 m
Total dam volume	3.61×10^6 m^3
Dam body materials' volume	1.7×10^6 m^3
Dam slope upstream	1:2.3 (V:H)
Dam slope downstream	1:2.1(V:H) + Berm
Total reservoir area	12.33 km^2

In this study, the recorded data from the instruments in the body of the dam are evaluated, along with the results of 3D numerical analysis. As indicated in Fig. 3, the Vanyar Dam has been instrumented in five cross-sections (i.e., A, B, C, D and E) along the dam. The main instruments installed for the monitoring system include magnetic settlement devices, vibrating pressure cells and vibrating wire piezometers. These instruments were installed along the three axes and various levels of the dam height. Pressure cells were installed in triple clusters in order to record total vertical stresses in three perpendicular directions. In this study, with regard to the approximate symmetry of the instrumented cross-section, valley profile, as well as the symmetry of the dam relative to the middle cross-section C, the instrumented cross-sections, including the critical cross-section C and the two cross-sections D and E, located in the right abutment of the dam, were evaluated. Fig. 4 shows the layout of the instruments in cross-sections C, D and E.

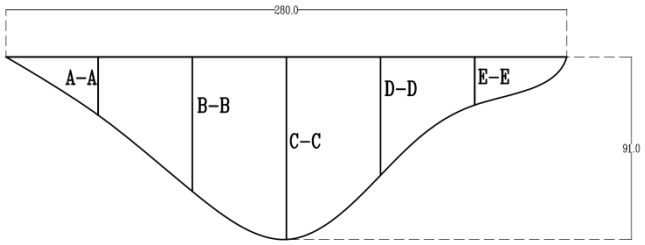

Fig. 3. Location of instruments in the five cross-sections on the longitudinal section of the rock-fill Vanyar Dam

The instrument data were recorded during the dam construction. For instance, Fig. 5 shows the variation in the total vertical stresses in the pressure cells at CPC16 in three perpendicular directions, i.e., σ_x, σ_y and σ_z. In addition, the variation in pore water pressure during the dam's construction at piezometer CVP10 is shown in Fig. 5. The instruments, whose data are shown in Fig. 5, are located in the core within the vicinity of the bedrock.

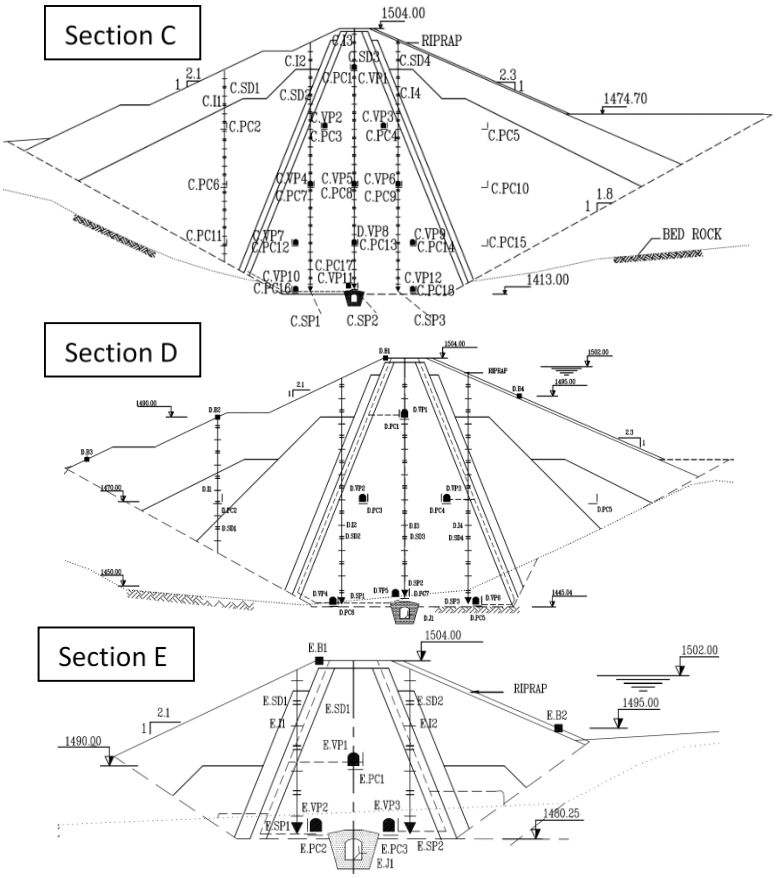

Fig. 4. Layout of the pressure cells, magnetic settlement detector and piezometers in cross-sections C, D and E [18]

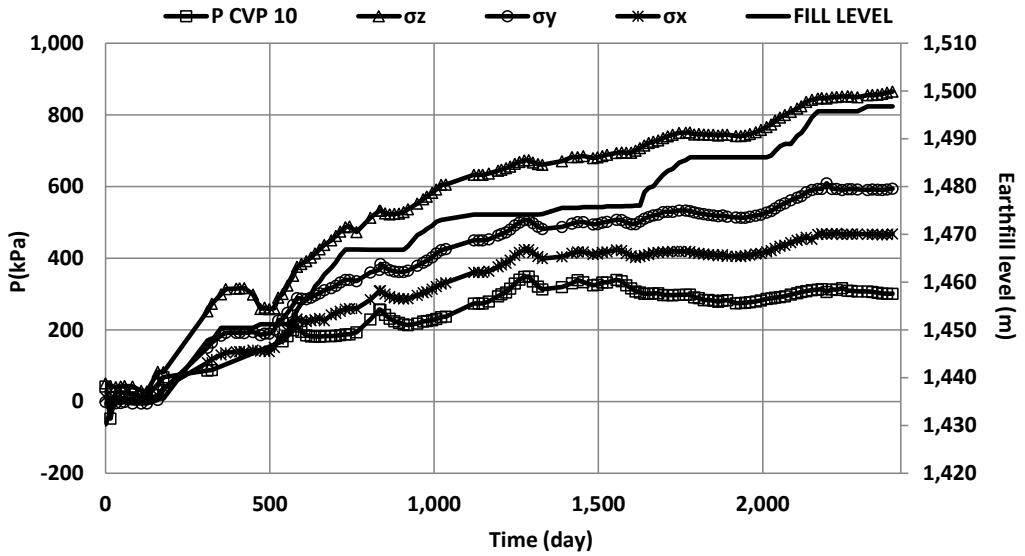

Fig. 5. Variation in total vertical stresses and pore pressure versus times for instruments CPC16 and CVP10 [18]

4. Numerical modeling

FLAC-3D software [19] was used to facilitate the numerical modeling of the Vanyar Dam at the end of construction. Many researchers used the software in order to 3D and 2D numerical analyses of earth dams and rock-fill dams ([20], [21], [22], [23]). It simulated the numerical calculation based on the finite difference method. The mesh generation in the dam body, as shown in Fig. 6, included 48,700 elements, which were considered for modeling. The boundary condition of the dam was extended 110 m, both upstream and downstream, and 50 m along the flanks of the dam crest. In addition, both sides of the dam were constrained against lateral displacements, while the bottom of the dam geometry was also constrained against both lateral and vertical displacements. To model the dam body for numerical calculation, the entire geometry of the dam body was first removed to simulate only the foundation, after which the initial stress in the foundation was calculated. Then, a finite difference layered analysis was performed by considering 18 layers in order to simulate the compaction during the dam construction. According to Clough and Woodward (1967), the stage construction of a dam body in the layers yields compatibility between reality and numerical modeling. The Mohr-Coulomb constitutive model was used to determine the material behavior of the dam and its foundation in the numerical analysis. The Mohr-Coulomb constitutive model was applied to analyze the rock-fill and earth dams by many researchers ([24], [25], [16]). The material properties, including friction angle (φ), cohesion (C), elasticity modulus (E), Poisson ratio (υ), dry density (γ_d) and permeability (k), were estimated by applying the laboratory and field tests on the resources, foundation and disposal materials. Table 2 shows the material properties of the dam body, alluvial foundation, bedrock and disposal.

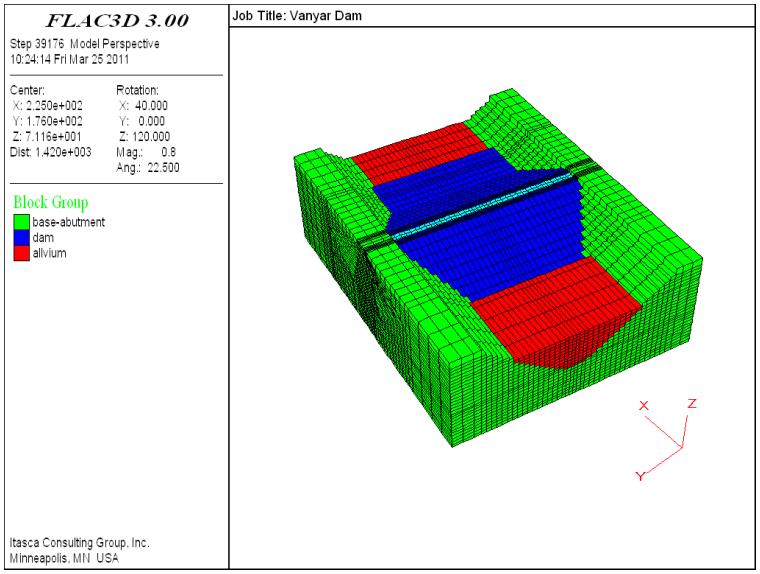

Fig. 6. Finite difference mesh for the body and foundation of the Vanyar Dam

Table 2: Material properties of the body, foundation and disposal of the Vanyar Dam [18]

Material	φ	C (kPa)	E (kPa)	υ	γ_d (kNm^{-2})	ψ	K (ms^{-1})
Clay core (CU)	30	15	20,000	0.35	20.1	1	5e-10
Filter	33	0	40,000	0.3	20	5	1e-5
Rock-fill shell	48	0	81,600	0.3	19.25	8	1e-4
Transient shell	42	0	60,000	0.3	20.25	7	5e-4
Foundation	30	20	35,000	0.3	19.5	2	1e-6
bedrock	50	60	390,000	0.27	22.5	8	1e-9
Disposal	28	0	30,000	0.3	19.5	0	1e-5

5. Results and discussion

In this section, the results of the 3D numerical analysis of the Vanyar Dam body are presented in terms of the settlements, total vertical stresses and pore water pressures.

5.1. Settlements

The settlements at the end of construction were evaluated in respect of three cross-sections (C, D and E). Fig. 7a shows the settlement contours in the largest cross-section (C) in the 3D model. Based on the settlement contours, the maximum settlement is 88.14 cm, which is located at the level of 48 m from the bedrock (z/H=0.75). In addition, Fig.

7b depicts the settlements along the longitudinal profile of the valley, which indicates that the maximum settlements were found at about the mid-height level, while the settlement contours are in good agreement with the geometry of the V-shape valley.

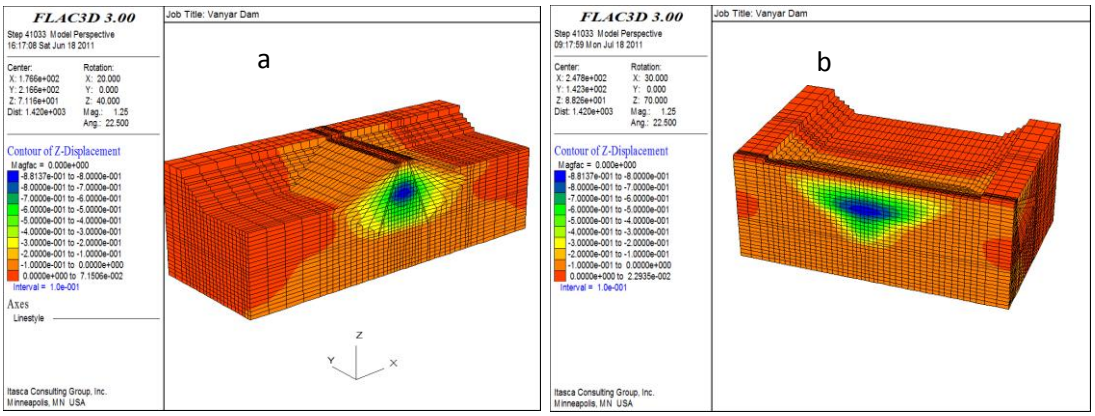

Fig. 7. Settlement contours at a) the largest cross-section (C) and b) along the longitudinal section of the dam crest

In Fig. 8, the results of the settlements obtained from numerical analysis are compared with data recorded by magnetic settlement detectors CSD3 and CSD4, which were placed with the instruments in the largest cross-section (C). This comparison is repeated for cross-sections D (DS3 and DS4) and E (ESD1 and ESD2) in Fig. 9 and Fig. 10, respectively.

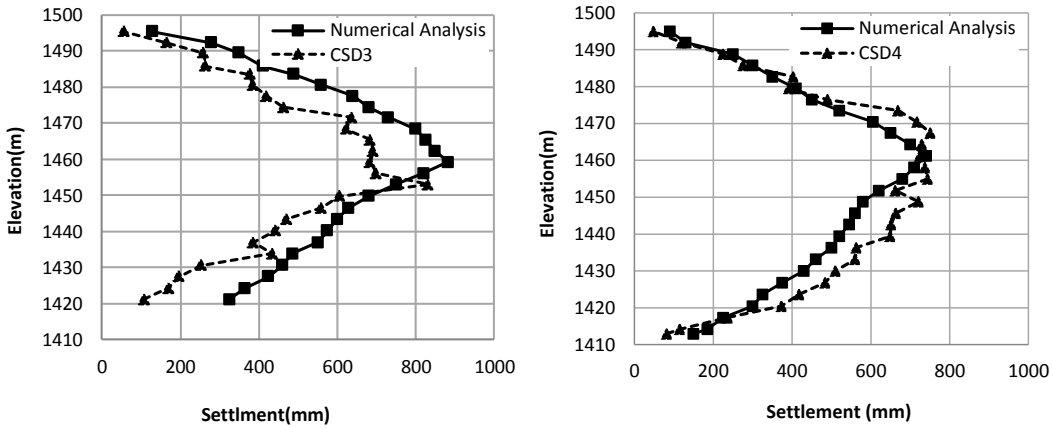

Fig. 8. Comparison of the settlements recorded by the instruments and the numerical analysis results for cross-section C

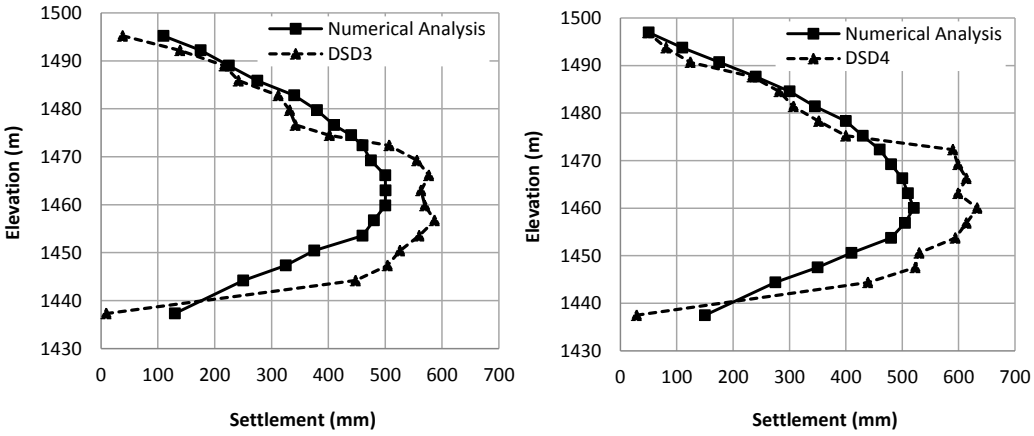

Fig. 9. Comparison of the settlements recorded by the instruments and the numerical analysis results for cross-section D

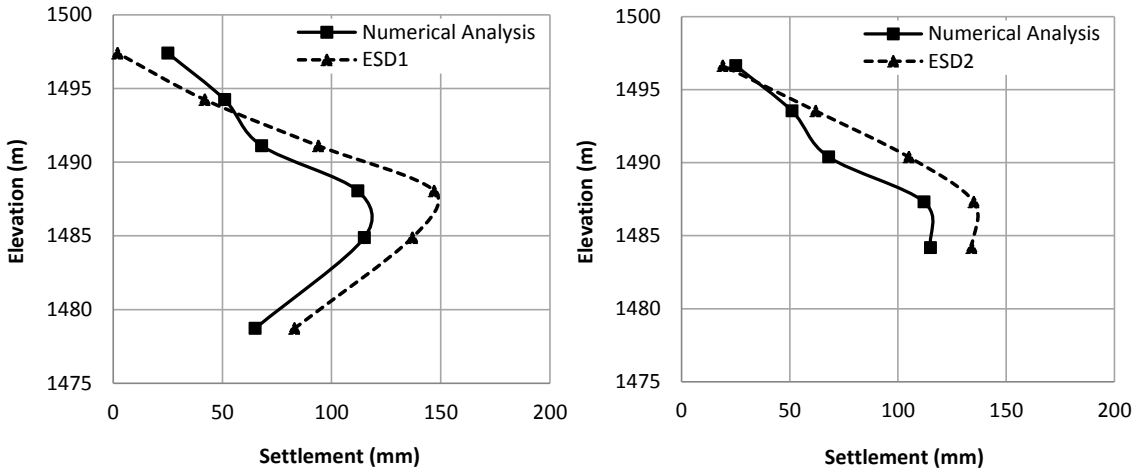

Fig. 10. Comparison of the settlements recorded by the instruments and the numerical analysis results for cross-section E

According to settlements recorded by the instruments and those obtained from the numerical analysis, the results are in good agreement. In addition, the results show that, except for CSD3, the settlements recorded by the instruments are greater than those obtained by numerical analysis. Lower compaction around the instruments, which prevented damage during compaction, created a lower stiffness area in the soil within the vicinity of the instrument that was not considered in the numerical modeling. Therefore, the settlements in the place of the instruments are greater than those obtained from numerical analysis. Fig. 11 depicts the simulation of the local arching around the instruments due to a lack of compaction.

According to the engineering consultant's report of the Vanyar Dam, CSD3 was installed at a later time than the other magnetic settlement detectors, which explains the contrasting behavior with other instruments. The low compacted soil around the instrument can be

assumed to have caused weak spring stiffness in the middle and the strong spring stiffness in the far end of the compacted soil. Therefore, under the same overburden pressure, the weak spring showed greater deflection than the strong spring. In this regard, Cetin et al. [26] illustrated that the significant settlement in the crest of Atatürk rock-fill dam in Turkey was due to lack of compaction in the core and slaking of weathered vesicular basalt rock-fill material.

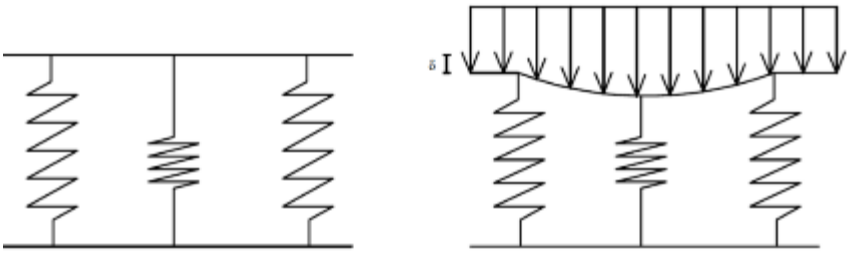

Before loading After loading

Fig. 11. Simulation of soil stiffness around the instruments

5.2. Total vertical stresses

The data recorded from the pressure cells are not sufficiently accurate because they are related to the soil compaction and construction process. Therefore, the total vertical stresses obtained from the numerical analysis verified those data instead [18]. The difference in the shear modulus in the various materials of the dam body reduced the total vertical stresses and created a local arching phenomenon in some areas of the dam. Maximum and minimum arching occurred around the filters and the middle of the core, respectively. The difference in the compressibility of the core and shell materials created a low-stress area in the core material in the vicinity of the shell. In other words, the vertical stresses transfer from the core to the shell. Furthermore, the reduction in the vertical stresses is more significant in the middle cross-section of earth dams, such that the overburden pressure (γh) is less than the vertical stresses in this area. During this process, horizontal cracks may appear due to the pore water pressure in the first impounding. This type of crack is called hydraulic fracturing. The arching phenomenon and, in turn, hydraulic fracturing are more probable in earth dams located in a narrow valley due to their local non-uniformity in the longitudinal section and the cross-section. Fig. 12a-b present the total vertical stress contours in the critical cross-section and

longitudinal section of the dam, respectively. In Fig. 12a, stress contours can be seen to conform to the dam geometry, while the arching phenomenon can be observed in the vicinity of the core and shell due to the difference in the stiffness of these two materials. Furthermore, gentle arching in the boundary of the alluvial and shell is visible. In Fig. 12b, the variation in the stress contour conforms to the dam's longitudinal section and the shape of valley. With respect to the narrow valley of the dam and the large difference in stiffness between the dam body and the foundation materials, the arching phenomenon can be see along the valley cross-section. This phenomenon is more significant at the lower level of the dam due to the narrowing of the valley.

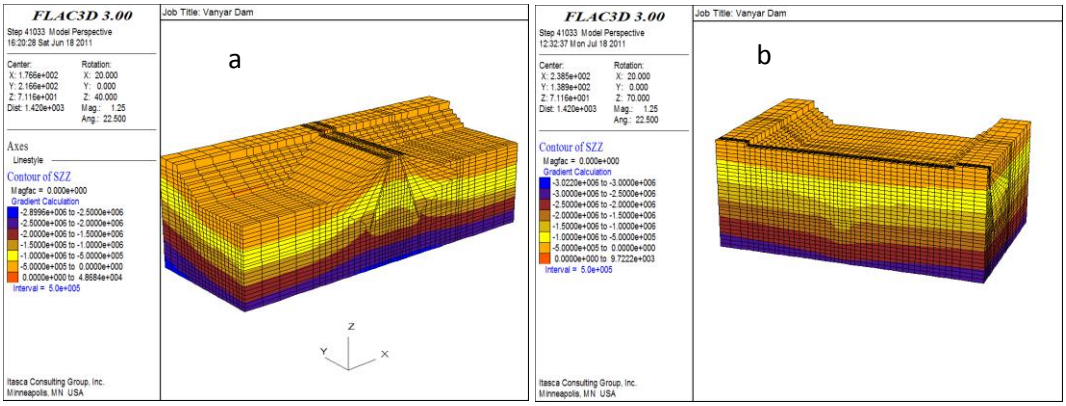

Fig. 12. Total vertical stress contours of a) cross-section C and b) the longitudinal section of the dam

In engineering practice, the arching is measured by the following equation:

$$A_r = \left(1 - \frac{\sigma}{\gamma h}\right) \times 100 \quad (1)$$

Where:

σ: The total stress at the point

γh: Moderate amount of overhead ground pressure at that point

Moradi et al., 2014 [27] conducted a series of numerical and statistical analyses on the various geometry of earth dam cross sections and suggested the following equations to evaluate the arching ratio:

$$for\ \frac{B}{H} \leq 0.5\ ,\quad A_r = -63.278\left(\frac{E_d}{E_r}\right) - 41.875\left(\frac{B}{H}\right) - 0.725(\alpha) + 105.441 \qquad (2)$$

$$for\ \frac{B}{H} > 0.5\ ,\quad A_r = -44.216\left(\frac{E_d}{E_r}\right) - 1.890\left(\frac{B}{H}\right) - 0.554(\alpha) + 71.712 \qquad (3)$$

Where:

B: Bottom width of the dam

α: Lateral aspect angle with the vertical axis of the dam

E_d: The elastic modulus of the dam

E_r: The elastic modulus of the dam foundation

For the cross-section C of the Vanyar Dam, B, H, α, Ed, and Er is about 92 m, 92m, 0.785 rad, 47,000 kPa, and 39,000 kPa, respectively. Therefore, Ar is calculated 64.1 % by using equation 3, while this value is determined 58.0% by equation 1. It shows that the proposed equations by Moradi et al., 2014 give a good estimation of the arching ratio.

In Fig 13, the variation in the total vertical stresses obtained from the numerical analysis is compared with the data recorded by the pressure cells along the height of the dam at the end of its construction. The results were obtained for cross-sections C, D and E from the dam axis, as shown in Fig. 13a-c, respectively.

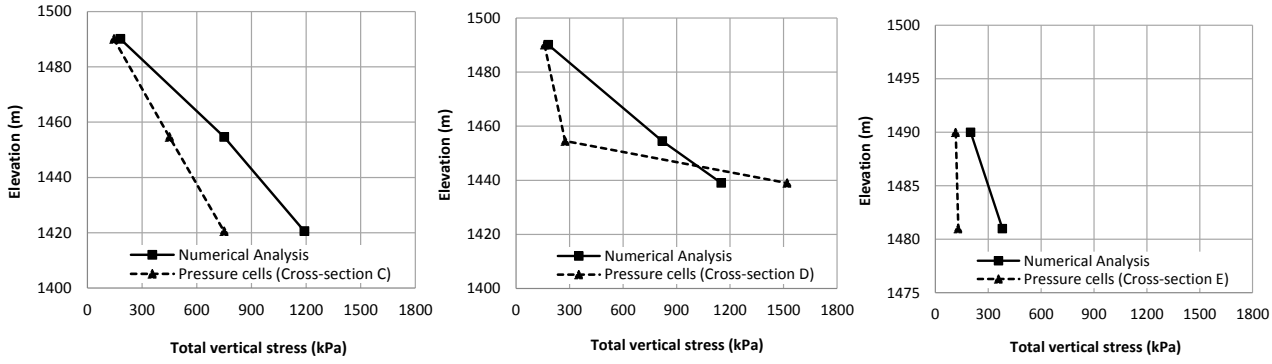

Fig. 13. Variation in the total vertical stresses obtained from the numerical analysis and the pressure cells along the height of the dam at the end of construction for cross-sections a) C, b) D and c) E

Fig. 14 shows the variation in the total vertical stresses obtained from 3D numerical analysis across the core at the middle cross-section for two elevations, i.e., h/3 and 2/3h. According to Fig. 14, there is a low-stress area around the boundary of the filter and core because of the arching phenomenon; other researchers have confirmed this kind of behavior [28].

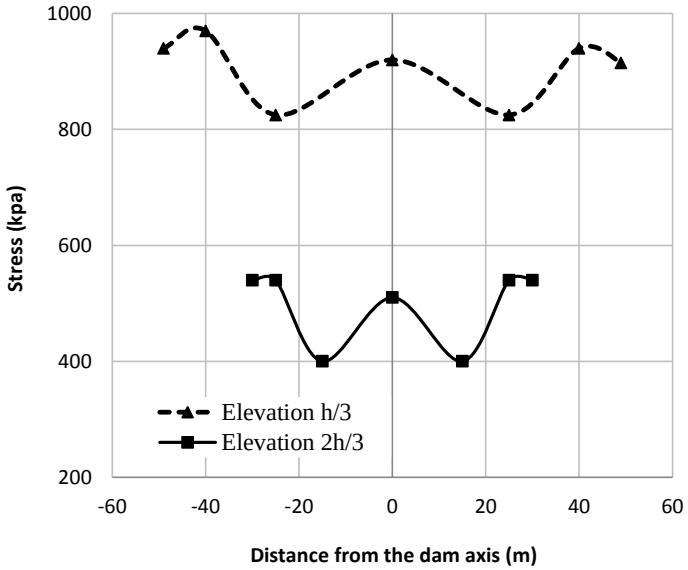

Fig. 14. Variation of vertical stresses cross the core at the levels of h/2 and 2h/3 of core in the cross-section C obtained from 3D numerical analysis

According to Fig. 13 and Fig. 14, most of the vertical stresses obtained from 3D numerical analysis were greater than those recorded by the pressure cells at that point. This may be due to the installation procedure for pressure cells. At the cell pressure installation stage, following maximum soil compaction, pressure cells are installed by digging a hole beneath and in the wall. Then, manual compaction is carried out in order to avoid damage to the pressure cells. Regarding the lower compaction around the pressure cells, in comparison to the compacted soil of the dam body, the vertical stresses from the numerical analysis are greater than those recorded by the pressure cells, due to local arching in the area of the pressure cells; meanwhile, in the numerical analysis, the core material is assumed to be homogeneous. After the consolidation of the integrated core, a reduction in the difference between the results of numerical analysis and the instruments is expected.

5.3 Pore water pressure

A realistic assessment of the pore water pressure in the core, during and after construction, shows that it affects the mechanical behavior of earth dams. Fig. 15a-b presents the pore pressure contours on cross-section C and the longitudinal profile of the Vanyar Dam, respectively. Fig. 15 also shows that the level of the water conformed to the

groundwater table of the riverbed at the end of construction. In addition, pore water pressure above the riverbed level at the core was dissipated and reached zero. Furthermore, pore pressures recorded by the piezometers confirmed this behavior.

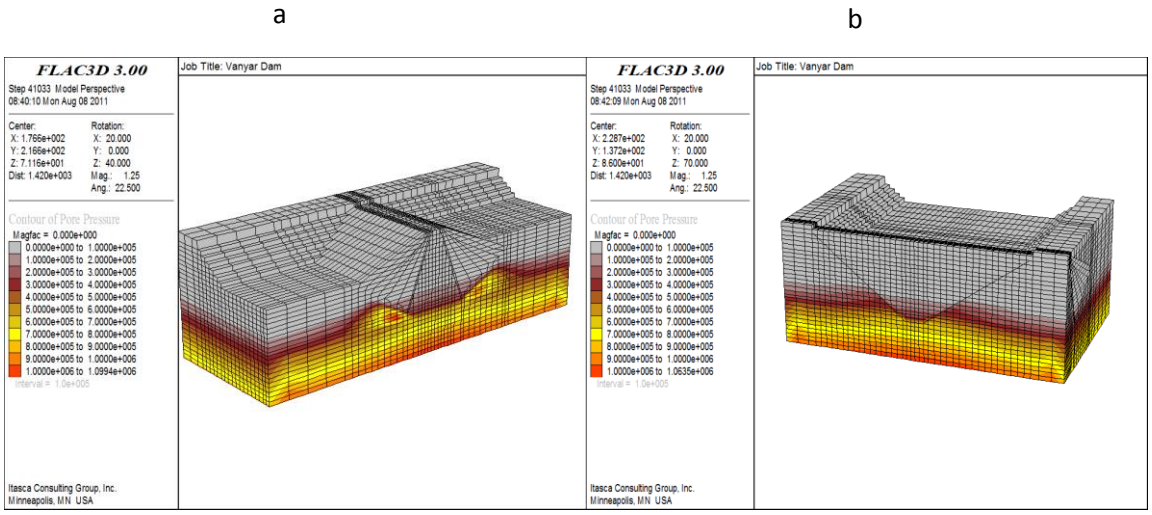

Fig. 15. Pore water pressure contours from 3D numerical analysis for a) cross-section C and b) the longitudinal profile of the dam

Fig. 16a-b shows the variation of pore water pressure along the height of the axis of the dam for cross-sections C and D. Both 3D numerical analysis and the piezometers show zero for cross-section E.

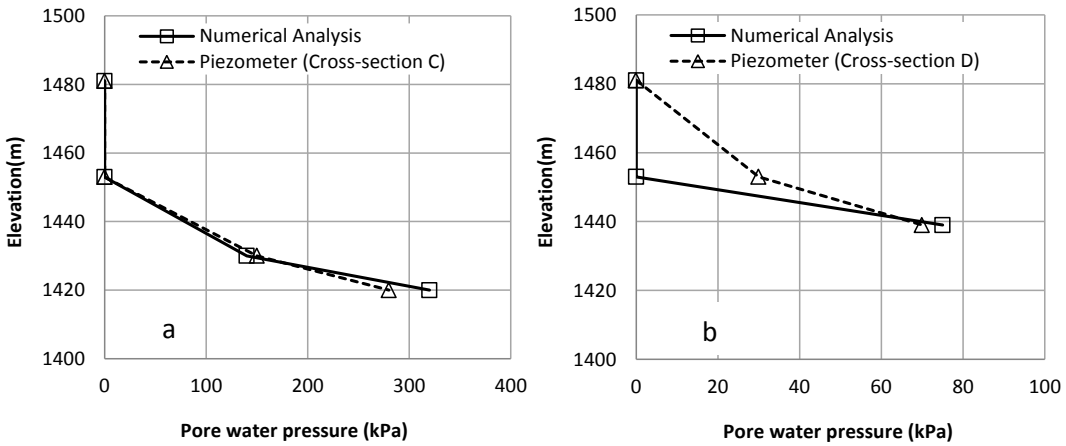

Fig.16. Variation in the pore water pressures obtained from the numerical analysis and pressure cells along the height of the dam at the end of construction for cross-sections a) C and b) D

The pore water pressure findings, as extracted by 3D numerical analysis and those recorded by the piezometers, are in relatively good agreement. Some of the piezometers, such as Cvp1 to Cvp6 and Evp1 to Evp3, located above the water table, with regard to the low permeability of the core and overburden pressures, showed no pore pressure. This could be due to the dissipation of the pore water pressures caused by the long-term construction of the dam (eight years). On the whole, the main reasons for the difference between the results of 3D numerical analysis and the data recorded by the instruments in terms of pore water pressures can be categorized as follows:

- According to the real geometry of the dam, the level of the groundwater table in the downstream area is lower than for the upstream area. For numerical modeling, the average of the groundwater table in the upstream and downstream areas was used. This simplification resulted in a small error, which led to a difference in the findings between the numerical analysis and instruments concerning pore water pressure.
- There was variation in the core material caused by the supply from different resources, which resulted in differences in the permeability of the core material. In addition, there were overburden pressure effects on the permeability of the core material, which was not considered by numerical modeling, resulting in some errors concerning pore water pressure within the findings of the numerical analysis.
- In reality, various areas of the dam body were not isotropic because the construction quality, weather conditions during construction of the soil layers, and dispersion of material properties in the dam body led to anisotropic behavior. Therefore, isotropic assumptions made in order to simplify the modeling of the materials resulted in some errors reported in the numerical analysis.
- The assumption about drainage conditions during the construction of the dam may not be entirely consistent with reality in the numerical modeling.

6. Conclusion

In this study, the results of the 3D numerical analysis of the Vanyar Dam, which is located in a fairly narrow valley, were compared with data recorded by the instruments installed

in the body of dam. The FLAC3D software was selected for numerical modeling of the dam. Settlements, total vertical stresses and pore water pressures were the three parameters that were evaluated by the results of the monitoring system and 3D numerical analysis. The results of this study include the following:

1. The settlements obtained by 3D numerical analysis were less than those recorded by the instruments. Light compaction around the instruments, in order to prevent damage to them during construction, is one of the most probable factors to explain this behavior. Based on 3D numerical analysis, the maximum settlement is about 88.1 cm, located 48 m above the bedrock in cross-section C, while the maximum settlement recorded by the instruments is 83.1 cm, located 41.9 m above the bedrock, which indicates that the settlements have made near-suitable adaptations and are both restricted to less than 1% of the dam height.
2. In terms of total vertical stresses, the pressure cells showed lower stress values in comparison to those obtained from the results of 3D numerical analysis. This may be due to local arching around the pressure cells because of light compaction of the core material around the pressure cells, which prevents damage to the instruments. The lack of accuracy concerning the installation angle of the pressure cells may also explain this difference. The average difference in the total vertical stresses between 3D numerical analysis and the data recorded by the pressure cells is about 28%, which is due to the aforementioned reasons.
3. The trend of the pore water pressures in the piezometers and the numerical analysis is fairly consistent. Some differences are due to a lack of accuracy in the modeling of the groundwater table, both upstream and downstream, the assumption that the permeability of the core material extracted from various areas of the material resources is the same, the consideration of the isotropic behavior for the materials in the body of the dam, and the lack of accuracy when simulating drainage conditions in numerical modeling. On the whole, the maximum adaptation between the results of the numerical analysis and the data recorded by the instruments was observed in the pore water pressure, meaning that the average difference between the results of the numerical analysis and the instruments was restricted to less than 1%.

According to the 3D numerical analysis results and their consistency with the data recorded by the monitoring systems for the three parameters (settlements, total vertical stresses and pore water pressures), the selected material properties, constitutive model and boundary condition are seemingly close to reality as recorded by the instruments. Therefore, it seems that 3D numerical analysis has been able to simulate the real behavior of the Vanyar Dam at the end of construction.

References

1. Eisenstein Z, Krishayya AVG, Morgenstern NR. An analysis of cracking in earth dams, USAEWES Vickburg.miss: 1972, p. 431–545.

2. Lefebvre G, Duncan JM, Wilson EL. Three-Dimensional Finite Element Analysis of Dams. J Soil Mech Found Div 1973;99(SM7):495–507.

3. Belyakov AA. Three-dimensional behavior of an earth dam at a wide site. Hydrotechnical Constr 1988;22:718–25. doi:10.1007/BF01429609.

4. Ohmachi T. A simpilified 3–D FEM and its application to dynamic of fill dam in narrow canyons Vienna, Austria, 17-21 June. Seventeenth Int. Congr. Large Dams, Viena: 1991, p. 165–78.

5. Stark TD, Eid HT. Performance of Three-Dimensional Slope Stability Methods in Practice. J Geotech Geoenvironmental Eng 1998;124:1049–60. doi:10.1061/(ASCE)1090-0241(1998)124:11(1049).

6. Javaheri H. Three dimensional dynamic analysis of Masjed-Soleyman rokfill dam. Sharif University of Technology, 1999.

7. Heidari T. The Comparison of Three and Two Dimensional Dynamic Analyses of Earth Dams. Iran University of Science and Technology, 2003.

8. Roth WH, Dawson EM, Somerville P, Davis CA, Plumb CC. Evaluation of the seismic performance of Stone Canyon dam with 2-D and 3-D analyses. 13 th World Conf. Earthq. Eng., 2004, p. 1–6.

9. Yu Y, Xie L, Zhang B. Stability of Earth-Rockfill Dams: Influence of Geometry on the Three-Dimensional Effect. Comput Geotech 2005;32:326–39.

10. Yu Y, Zhang B, Yuan H. An intelligent displacement back-analysis method for earth-rockfill dams. Comput Geotech 2007;34:423–34.

11. Qu G, Hinchberger SD, Lo KY. Case studies of three-dimensional effects on the behaviour of test embankments. Can Geotech J 2009;46:1356–70.

12. Mahinroosta R, Alizadeh A, Gatmiri B. Simulation of collapse settlement of first filling in a high rockfill dam. Eng Geol 2015;187:32–44. doi:10.1016/j.enggeo.2014.12.013.

13. Maddah A, Soroush A, Tabatabaie Shourijeh P. EEects of material properties on behavior of embankment dam clay cores in narrow valleys. Sci Iran A 2015;22:1692–702.

14. Gurbuz A, Peker I. Monitored Performance of a Concrete-Faced Sand-Gravel Dam. J Perform Constr Facil 2016;30:4016011. doi:10.1061/(ASCE)CF.1943-5509.0000870.

15. Sukkarak R, Pramthawee P, Jongpradist P. A modified elasto-plastic model with double yield surfaces and considering particle breakage for the settlement analysis of high rockfill dams. KSCE J Civ Eng 2016:1–12. doi:10.1007/s12205-016-0867-9.

16. Derakhshandi M, Pourbagherian HR, Baziar MH, Shariatmadari N, Sadeghpour AH. Numerical analysis and monitoring of a rockfill dam at the end of construction (case study: Vanyar dam). Int J Civ Eng 2014;12:326–37.

17. Mansouri H, Jorkesh Z, Ajalloeian R, Sadeghpour AH. Investigating effects of water salinity on geotechnical properties of fine-grained soil and quartz in a sandstone case study: Ajichay project in northwest Iran. Bull Eng Geol Environ 2017;76:1117–28. doi:10.1007/s10064-016-0920-4.

18. Ghodsniroo Engineering Co. Technical reports of Vanyar dam. Tehran: Ghods-Niroo consultant engineers Co.; 2011.

19. ITASCA. No Title. FLAC3D Version 30, Fast Lagrangian Anal Contin 3 Dimens 2005.

20. Bergado DT, Teerawattanasuk C. 2D and 3D numerical simulations of reinforced embankments on soft ground. Geotext Geomembranes 2008;26:39–55. doi:10.1016/J.GEOTEXMEM.2007.03.003.

21. Stark TD, Beaty MH, Byrne PM, Castro G, Walberg FC, Perlea VG, et al. Seismic deformation analysis of Tuttle Creek Dam. Can Geotech J 2012;49:323–43. doi:10.1139/t11-107.

22. Qi C, Lu W, Wu J, Liu X. Application of Effective Stress Model to Analysis of Liquefaction and Seismic Performance of an Earth Dam in China. Math Probl Eng 2015;2015:1–7. doi:10.1155/2015/404712.

23. Clough RW, Woodward RJ. Analysis of embankment stresses and deformations. J Soil Mech Found Div 1967;93(SM4):529–49.

24. Gharti HN, Komatitsch D, Oye V, Martin R, Tromp J. Application of an elastoplastic spectral-element method to 3D slope stability analysis. Int J Numer Methods Eng 2012;91:1–26. doi:10.1002/nme.3374.

25. Ke W, Mingyue M, Dongxue H. Numerical analysis on mechanics of interaction between slurry and soil in earth dam by splitting grouted. Elsevier 2012;28:351–5.

26. Cetin H, Laman M, Ertunç A. Settlement and slaking problems in the world's fourth largest rock-fill dam, the Ataturk Dam in Turkey. Eng Geol 2000;56:225–42. doi:10.1016/S0013-7952(99)00049-6.

27. Moradi M, Shirgir V, Ghanbari A. An approximate equation for the estimation of arching due to the shape and hardness of valley in earth dams. Electron Journal of Geotechical Engineering; 19: 6343-6352.

28. Hunter GJ. The Pre-and Post-Failure Deformation Behaviour of Soil Slopes. The University of New South Wales, 2003.